An Adaptive MAC-Agnostic Ranging Scheme for Underwater Acoustic Mobile Networks

Antonio Montanari, Filippo Campagnaro, Michele Zorzi

[a] *University of Padova, Department of Information Engineering (DEI), via Gradenigo 6/b, Padova, 35131, PD, Padova*

Abstract

In the last ten years several simulation studies on Autonomous Underwater Vehicle (AUV) swarm fleet formation have been performed, and some preliminary sea demonstrations of proof-of-concept prototypes were carried out. However, their actual realization is hindered by the challenges imposed by the underwater acoustic channel and the difficulties of keeping track of the vehicles' positions due to the long latency required by traditional Two-Way Travel-Time (TWTT) ranging measurements, that require a specific signalling, hence limiting the throughput of the underwater network. Although One-Way Travel-Time (OWTT) halves the latency, it requires a high precision oscillator, such as an atomic clock or an oven controlled crystal oscillator (OCXO), to be installed in each modem processing unit: while atomic clocks are still very expensive, OCXO are very power demanding, making their application to underwater acoustic networks not always possible, especially in the case of low cost vehicle swarms.

In this paper we present a network protocol stack able to perform ranging and localization within the communication task in underwater acoustic networks, limiting the network overhead. Specifically, new layers have been added to the preexisting DESERT Underwater protocol stack to perform the ranging tasks without compromising the correct operation of the communication network. A ranging layer is placed on top of the Medium Access Control (MAC) scheme, allowing the latter to be changed according to the network topology and requirements. This MAC-agnostic ranging layer is further optimized by adapting the amount of data transmitted according to the channel state, and the ranging entries inserted in the data packets according to the least recent information transmitted, hence minimizing the Age of Information. Simulation results obtained with the DESERT Underwater Framework show how this layer allows all AUVs in the swarm to know their distance from every other node in the network, thus limiting the probability of vehicle collisions and allowing better mission coordination.

Keywords: Underwater acoustic networks; ranging in underwater networks; DESERT Underwater Framework; network simulation; age of information; value of information.

1. Introduction and state of the art

The recent availability of low cost underwater vehicles as either commercial products [1] or open source projects [2] is encouraging their deployment in swarms of Autonomous Underwater Vehicles (AUVs) (Figure 1) to enable a wide range of civilian applications, from submarine scientific explorations to environmental monitoring [3]. A key requisite for any AUV task is location awareness which cannot be obtained by means of Global Navigation Satellite System (GNSS), due to the unavailability of this signal underwater. Classical underwater positioning or ranging methods rely on measuring either the one-way or the return travel time of acoustic signals between the vehicles: One-Way Travel-Time (OWTT) ranging is possible when all the vehicles share a common time base, which requires the on board presence of high precision clocks such as a Chip Scale Atomic Clock (CSAC) [4], or a less expensive but less accurate Oven-Controlled Crystal Oscillator (OCXO) [5]. Two-Way Travel-Time (TWTT) ranging instead does not require node synchronization, at the cost of doubling the latency and the number of messages exchanged to measure each distance.

The challenges imposed by the underwater acoustic channel [6, 7, 8], including poor performance in shallow water due to strong reverberation, long propagation delay, low bitrate and high dependence on weather conditions, make localization and communication tasks even more difficult. In fact, other existing communication technologies, such as magneto-inductive, optical, and

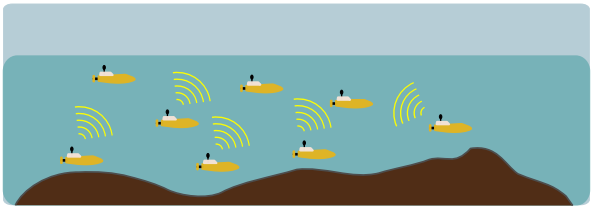

Figure 1: Coordinated AUV swarm formation.

radio frequency, can be used only for short range communication links, up to a few tens (optical and RF), or a few hundreds (magneto-inductive) of meters [9], making acoustic communication the only one able to establish long range links.

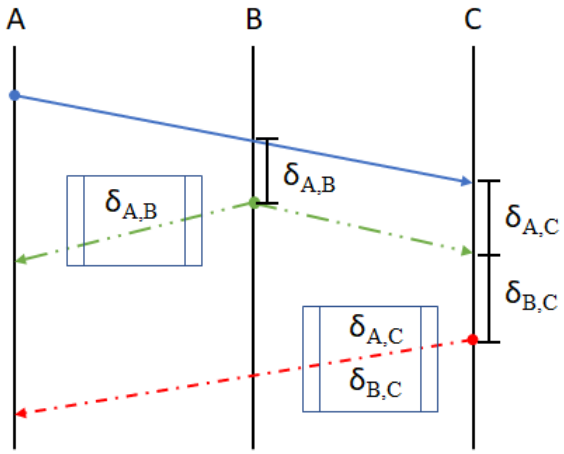

Figure 2: Hyperbolic ranging message exchange between nodes A, B, C

Upon these basic principles, different ranging/positioning schemes can be developed according to the use case scenario. This paper, which significantly expands and enhances our previous work [10], relates to a scenario where, in a swarm of N AUVs, each vehicle is required to know not only the distances from itself to the other $N-1$ nodes, but also the distances between all the other nodes. This knowledge itself could be used to optimize the communication protocol [11], or, in case some of the nodes are used as fixed references, to calculate the absolute positions of the vehicles in the swarm, by forming a Distributed Long BaseLine (DLBL) [12, 13]. In contrast to traditional ranging and communication systems, such as Long, Short, and Ultra Short BaseLine (LBL, SBL, and USBL) [14, 15], the proposed system does not require specific hardware (unlike USBL) or the presence of many anchors (unlike LBL and SBL) in addition to the acoustic modems installed in the nodes of the network, significantly lowering the deployment cost and complexity [13, 15]. We consider in particular the "hyperbolic" ranging scheme first presented in [16] and then further cited in [17] and [12], where it was implemented and evaluated upon a Time Division Multiple Access (TDMA) Medium Access Control (MAC) protocol. In this scheme (Figure 2), each node cyclically broadcasts a ranging packet which embeds the $N-1$ time differences measured from the transmission instant of said packet to the respective time of reception of each of the $N-1$ packets which were broadcast by the other nodes. At the end of each cycle each node would have collected enough information ($N \cdot (N-1)$ equations) to calculate all the required $D = \frac{N \cdot (N-1)}{2}$ distances. One contribution of this paper is to present not only the working principles, but also a detailed implementation of the scheme, enhanced with data reduction features that will be outlined in the following sections. This data reduction does not only adapt the packet size according to the observed channel conditions, but also selects the value being transmitted to minimize the Age of Information (AoI) [18]: simulations proved that this approach outperforms other transmission policies and is one of the main contributions of this paper. This implementation has been included in the DESERT Underwater framework, a publicly available[19] underwater network simulation and experimentation tool developed and maintained by the SIGNET group at the University of Padova [20].

Another interesting aspect is the analysis of which MAC protocol performs best in a ranging scheme. In [21], for instance, the authors show that a contention-based MAC can outperform a contention-free MAC when referring to ranging precision in underwater networks: these results highlight the importance of selecting the most suitable MAC protocol for the analyzed network topology, hence developing a ranging scheme that depends on a specific MAC will limit the use of such a system only to a few specific topologies. Therefore, the second contribution of this paper is to present a ranging protocol for underwater networks that is agnostic to the MAC used by the network. Nevertheless, since the choice of the underlying MAC has a non negligible impact [12, 22] on the performance of the ranging scheme, we perform a comparison of the ranging precision over TDMA, CSMA-Aloha and Tokenbus under varying parameters, configurations of the swarm, and channel conditions. `TokenBus` [23] is a round-robin contention-free MAC that forms a logical ring topology, where only the node with the token can transmit: after transmitting it passes the token to the next node in the ring (the token can be piggybacked in a data packet): the implementation of a `TokenBus` protocol for underwater

networks is presented in [10]. TDMA, instead, is a well-known contention-free MAC protocol where the time is divided in time frames, each composed of as many time slots as the number of nodes in the network: in each slot, only one node can transmit. The use of TDMA in underwater networks may cause interference between nodes transmitting in subsequent time slots due to the long propagation time: to mitigate this effect, a large guard time between slots needs to be used. Finally, CSMA-Aloha is a carrier-sense contention-based MAC protocol. The implementation of the three protocols is available at [19].

The rest of the paper is organized as follows. Section 2 describes the ranging protocol, and Section 3 presents its cross-layer implementation in the DESERT stack. Section 4 depicts the simulation scenarios, while Section 5 discusses the results and the ranging performance. Finally, Section 6 concludes the paper.

2. Protocol description

In this section we describe the distributed ranging protocol developed in this paper, form here onward referred as UwTDOARanging. We recall that this protocol implements the "hyperbolic" ranging scheme depicted in Figure 2. Specifically, each node cyclically broadcasts a ranging packet which embeds the $N-1$ time differences measured from the transmission instant of said packet, to the respective time of reception of each of the $N-1$ packets which were broadcast by the other nodes. At the end of each cycle each node would have collected enough information to calculate all the required distances.

In details, the UwTDOARanging protocol works on this principle: each node generates ranging packets according to a deterministic or a stochastic process with a generation rate of mean λ. Each packet is sent down to the MAC to be broadcast according to the MAC scheduling policy. Whenever a node C receives ranging packets from other nodes $A, B, \ldots$, it saves locally their arrival times Tr_A, Tr_B.... Eventually, node C will decide to broadcast its own ranging packet, including in the payload all the holdover times $\delta_{x,C}$ from each arrival time until the instant of transmission Tt_C: $\delta_{A,C} = Tt_C - Tr_A$, $\delta_{B,C} = Tt_C - Tr_B$, ...; the instant of transmission Tt_C is saved locally as well. When this packet is received by node A at local time Tr_C, A is able to calculate right away the Round Trip Time (RTT), and thus an approximation of the distance

$$\widehat{dist_{A,C}} = \frac{Tr_C - Tt_A - \delta_{A,C}}{2 \cdot s_{sp}}. \quad (1)$$

Furthermore, having received at time Tr_B the packet previously sent by node B, carrying the value δ_A computed by B, node A is able to estimate at once also the distance

$$\widehat{dist_{B,C}} = \frac{Tr_C - Tr_B - \widehat{dist_{A,B}} + \widehat{dist_{A,C}} - \delta_{A,C}}{2 \cdot s_{sp}}. \quad (2)$$

It should be noted that in a network of N nodes, each packet can contain up to $N-1$ δ_x values, so when correctly received each node can update a target distance according to equation (1) and $N-2$ distances according to equation (2). This means that in a cycle any node A will update a distance $\widehat{dist_{B,C}}$ regarding any other nodes B and C twice: upon both reception of a packet from B and from C. This fact, along with the understanding that sending ranging packets with $N-1$ entries will make the packet size scale linearly with the number of nodes in the network, suggests that a policy for reducing the number of entries in the packet payload could be put in place in case of packet size constraints, to improve the Packet Delivery Ratio (PDR) according to the channel conditions, to save on energy spent for transmission and to lower the channel occupation. Moreover, according to the specific task assigned to the nodes forming the swarm, there could be clusters of nodes with different requirements on the ranging accuracy, so a node could include more often entries involving the peers in the cluster in its ranging packets. The notation is summarized in Table 1.

3. Protocol Implementation

In this section we present how the ranging protocol has been implemented in the DESERT framework. As depicted in Figure 3, the UwTDOARanging ranging module is placed upon the MAC module: it generates ranging packets that are sent to the MAC to be transmitted according to its own policy.

3.1. Packet structure

The packet structure is shown in Figure 4 and it includes a header with a NodeId (5 bits) and a PktId (3 bits) field. The former is needed to identify the node sending the packet in a swarm of up to 32 nodes, whereas the purpose of the latter is to avoid the possibility that two ranging packets from the same node get aliased. This can happen when a ranging packet is correctly received by some nodes but lost by others: if a discriminatory header field is not present, the two

Table 1: Notation and meaning

Notation	Meaning
λ	ranging packets generation rate
Tr_x	instant of reception of a ranging packet transmitted by node x
Tt_y	instant of transmission of a ranging packet by node y
$\delta_{x,y}$	holdover time calculated by a node y as $Tt_y - Tr_x$
$\widehat{dist}_{x,y}$	estimated distance from node x to node y
$\widehat{dist}_{x,y}(t)$	estimated distance from node x to node y computed at time t
s_{sp}	sound speed underwater ($\simeq$1500 m/s)
N	number of nodes
TT	travel time
J	holdover jitter introduced by the MAC
$S(k)$	size of a packet in bytes with k entries, in bytes, computed as $S(k) = 1 + 3 \cdot k$
TRT	token rotation time in a token-ring network
$G_{Ns}(k)$	global goodput expected by node N_s
	if k entries are transmitted
N_s	transmitting node
N_d	receiving node
D	number of distances each node computes
PER, BER	packet error rate, bit error rate
$RMSE$	root mean square error

groups of nodes will then send packets with Time Difference Of Arrivals (TDOA) entries referring to different packets sent at different times, resulting in inconsistent measurements. The payload of the packet contains a variable number of entries, each carrying a holdover time, i.e., the time elapsed from the reception of a certain packet (`NodeId`, `PktId`), until the transmission of the current packet. It is evident that each entry has to be identified by a couple (`NodeId`, `PktId`) to be associated to the corresponding packet. Since a packet has a 1 byte header and each entry itself has a 1 byte header plus 2 bytes for the holdover time, for a packet with k entries the resulting size is therefore $S(k) = 1 + 3k$ bytes.

3.2. Stack

As described in Sec. 2, this ranging protocol is designed to work without relying on a particular underlying MAC policy, however, it still needs precise reception and transmission timestamps. We achieved this by interposing a "TAP" layer, named `UwTAP`, between the MAC and the physical layer: when a ranging packet is passed down by the MAC, the `UwTAP` withholds the packet and notifies the `UwTDOARanging` to allow the update of the holdover times in all the entries to the actual

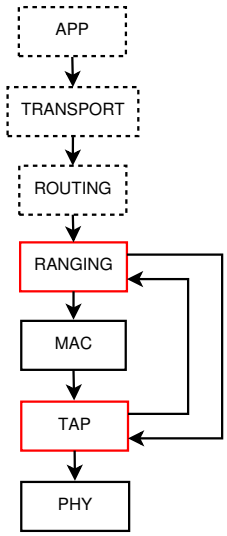

Figure 3: Stack of a node: Ranging and TAP modules are the contribution of this paper. Although ranging packet can be transmitted along with data packets generated by the higher layers, in this work we focus on the ranging protocol.

transmission time. To accomplish this, each packet is associated with a timestamp which holds the generation epoch: this epoch is used by `UwTDOARanging` and not transmitted over the channel. When `UwTDOARanging` is notified that the packet is being passed to the physical layer for being actually transmitted, `UwTDOARanging` adds to each `HoldoverTime` the time elapsed since the generation timestamp, so that the holdover times reflect the time from reception to the actual transmission. `UwTDOARanging` has been placed right on top of the MAC layer, so the ranging packets are not burdened with other protocol headers. Furthermore, this could allow opportunistic policies such as piggybacking a range packet to outgoing data coming from upper layers, instead of generating them according to an independent process. In this implementation, however, both `UwTAP` and `UwTDOARanging` layers are completely transparent to data packets and service requests generated by other layers: such data is simply relayed through the `UwTAP` and `UwTDOARanging` modules.

3.3. Generation policy

In this implementation, the user can choose to generate ranging packets according to a fixed period $T = 1/\lambda$. The λ parameter ideally should be as high as possible to limit the AoI of the distance measures. In fact the error on the distance between a pair of nodes A, B, which is the difference between the distance calculated by the ranging protocol at a certain time T_0 and the true dis-

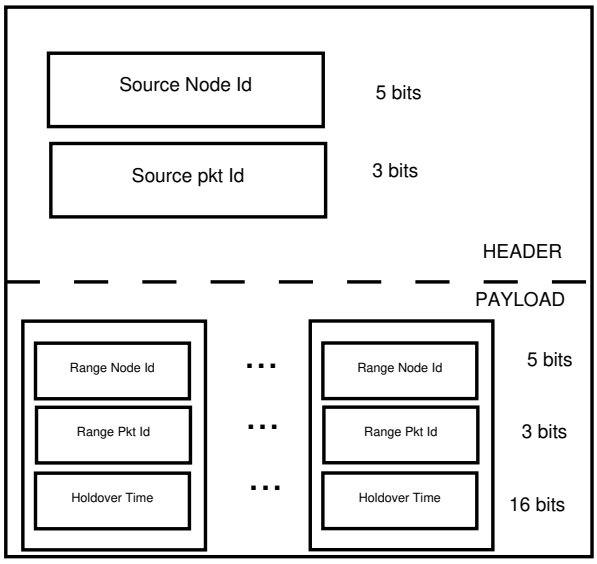

Figure 4: Ranging packet structure.

tance at a given time T_1 is given by

$$e = \int_{T_0}^{T_1} |\mathbf{v}_A - \mathbf{v}_B| \, dt \tag{3}$$

being $\mathbf{v}_A$ and $\mathbf{v}_B$ the respective instantaneous node speeds and $T_1 - T_0$ the AoI associated to the distance measure. Since the maximum AoI is proportional to the period of the ranging packet generation $1/\lambda$, it is clear that, the higher the node speed, the higher λ should be to obtain the same ranging performance. In practice, λ has to be set considering channel bandwidth, coexisting data traffic and underlying MAC policy. When considering a TDMA scheme, it would be of no use to have multiple ranging packets sent in the same time slot and conveying the same information, so the maximum useful value for λ is such that $1/\lambda$ is equal to the frame period T_f, which has to be long enough for the transmission of one ranging packet plus the data from other applications. In this case, being T_g the guard time after each slot, B the channel bitrate, k the number of nodes and $S(k)$ the ranging packet size, the ranging scheme will occupy a fixed fraction of the maximum available throughput which can be expressed by

$$\frac{\min(1, \lambda \cdot T_f) \cdot S(k)}{B \cdot (T_f/k - T_g)} \tag{4}$$

For the same reason, when using a token-ring MAC, $1/\lambda$ should not be shorter than the Token Rotation Time (TRT), which is not a fixed value, but depends on the propagation times between consecutive nodes in the ring. Considering all the dynamics that can influence the effectiveness of λ might lead to choosing a conservative value that fits for the worst traffic and latency scenario. A one-fits-all solution we proposed in this implementation consists in allowing only one ranging packet to be present in the outgoing queue at any time, so the generation of new ranging packets is inhibited until `UwTDOARanging` is notified by `UwTAP` that the packet already in the queue has been sent. This allows setting a high λ value which in slotted MACs will guarantee a ranging packet is present in each slot in order to maximize the ranging performances at the expense of bandwidth occupation.

3.4. Variable packet size policies

A node can choose to include a number of entries $k < N - 1$ in the ranging packet, reducing its size according to channel condition and network load. In this work, we tested some adaptive policies with the goal of reducing the ranging packet size while minimizing the error on the distance measurements. In order to do this we make the assumptions that:

- the channel between each pair of nodes (N_s, N_d) is symmetric and slow varying;
- every node N_t can make some estimate of each channel's Bit Error Rate (BER) $BER(N_t, N_r)$ from the Received Signal Strength Indicator (RSSI) or output Signal to Noise Ratio (SNR) of the last packet received from each node. If the modem is not able to perform this estimate, we assume that at least the instantaneous PDR can be computed, from which the BER can be roughly estimated.

Without loss of generality, in the next analysis we do not consider channel coding: nevertheless, the following formulas can be modified for any modulation and coding scheme. With these assumptions the node about to transmit can estimate the Packet Error Rate (PER) for each receiving node N_d and packet size $S(k)$ as

$$PER(N_s, N_d, k) = (1 - BER(N_s, N_d))^{8 \cdot S(k)}, \tag{5}$$

and then for every possible value of $k = 1 \ldots N - 1$ it takes the first k nodes with the best SNR and computes their expected aggregate PDR as per Eq. (6)

$$G_{N_s}(k) = \sum_{\substack{N_d=1 \\ N_d \neq N_s}}^{k} (1 - BER(N_s, N_d))^{8 \cdot S(k)}, \tag{6}$$

so the optimal value K is chosen as

$$K = \arg\max_k G_{N_s}(k). \tag{7}$$

Once K is set, the sending node N_s has to choose which entries shall be included in the outgoing packet, i.e. to choose for which NodeIds the holdover value will be included in the packet.We tested two different policies: the first, from now on named B-SNR, is based on the selection of the entries involving the nodes with the best SNR, and the second, named AoI, is based on an AoI metric. We compare them with the benchmark "Full Packet" policy. The three policies are better described as follows.

- "B-SNR" policy selects the first K entries for which the SNR of the channel between the sender and the node associated with the entry NodeId have the highest values, so that the nodes that maximize the expected global goodput of Eq. (6) are those who will receive the information for updating their Two-Way Ranging (TWR) distance measurements.
- "AoI" policy aims to minimize the AoI metrics, that in this paper is calculated by N_s for each receiving `NodeId` as the time elapsed since it last sent an entry with a `NodeId` label. In this approach, the K entries that accumulated the largest AoI are sent: this is equivalent to choosing the `NodeIds` from a circular queue which consumes K entries per round.
- "Full" packet policy simply does not apply any adaptation, and always transmits packets with the maximum size (hence containing all $N-1$ entries).

4. Simulation Scenario and Settings

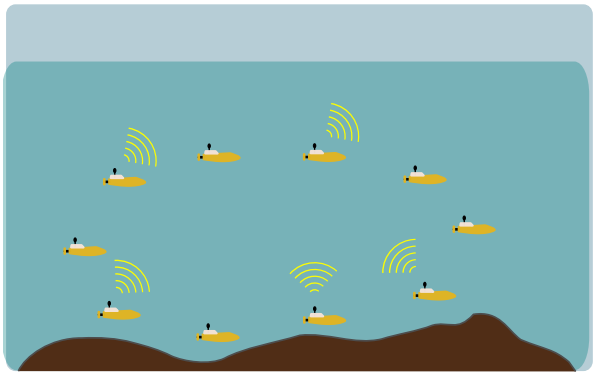

Figure 5: Simulation scenario and nodes deployment at the beginning of the mission.

In our first scenario the goal was ranging efficiency, i.e., trying to keep the ranging performance while reducing the size of the packet sent. As performance metric we chose the time series of the Root Mean Squared Error (RMSE) calculated for each node over the measured distances (Eq. (8)),

$$\text{RMSE(n, t)} = \sqrt{\frac{1}{D}\sum_{d=0}^{D-1}\left(\widehat{dist_{d,n}(t)} - dist_{d,n}(t)\right)^2}, \quad (8)$$

where $\widehat{dist_{d,n}(t)}$ is the distance calculated by node n at time t and $dist_{d,n}(t)$ is the true distance value. The distances are sampled every 5 seconds and compared to the true distances, assuming for the calculations a fixed sound speed of 1500 m/s and that multi path is absent or taken care of by the Physical layer. The distance measurements are raw and no filtering or prediction mechanism is applied.

4.1. Nodes movement pattern

We tested the `tdoa_ranging` implemented in the DESERT framework with 10 nodes initially equally spaced along a circle of 10 m diameter. The nodes then start moving according to 7 phases: during even phases (0,2,4,6) nodes drift in a radius of 10 m around the initial position or the target position they have reached during phases (1,3,5). During odd phases nodes move radially expanding from the current to the target positions which are equally spaced along circles of diameter respectively of 100, 500, 1000 m. During both drift and radial movement each node has a speed of 1 m/s. To help the reader, the phases are summarized in Table 2. This movement pattern allows to have a view of the different response of `UwTDOARanging` with both linear and random movements of the nodes over different MAC schemes and at different ranges.

Table 2: Movement phases

Phase	Description
0	nodes equally spaced along a 10 m-diameter circle, drift in a radius of 10 m around their initial position
1	nodes move radially to reach a circumference with a diameter of 100 m
2	nodes equally spaced along a 100 m-diameter circle, drift in a radius of 10 m around their initial position
3	nodes move radially to reach a circumference with a diameter of 500 m
4	nodes equally spaced along a 500 m-diameter circle, drift in a radius of 10 m around their initial position
5	nodes move radially to reach a circumference with a diameter of 1000 m
6	nodes equally spaced along a 1000 m-diameter circle, drift in a radius of 10 m around their initial position

4.2. Simulation settings

The simulated network stack, presented in Figure 3, is tested with three different MAC layers, namely: `TokenBus`, `TDMA` and `CSMA-Aloha`. The three protocols are configured as follows.

- `TokenBus`: the slot time Tk_{slot}, which in the TokenBus standard terminology [10] is the maximum RTT between two nodes, is set to 1.6 s, corresponding to a maximum distance of 1200 m;
- `TDMA`: the guard time (t_g) between TDMA slots is set to 0.15 s as lower values led to a high number of packet collisions in the simulated setup as shown in Figure 10, the frame duration (T_f) is set to 2.5 s so that each node has a Tk_{slot} of 0.1 s sufficient for transmitting 64 bytes at the bitrate of 5120 bps plus the t_g;
- `CSMA-Aloha`: the channel listening time is uniform from 0 to 0.5 s plus a 0.25 s constant.

The maximum ranging packet size is 30 bytes: a smaller packet size can be used if the adaptive algorithm is activated (as described in Section 3.4).

Table 3: Simulation settings

Parameter	Value
Number of nodes (N)	10
Source level	170 dB re 1 μPa 1 m
Water depth	200 m
Central frequency	65 kHz
Bandwidth	30 kHz
Bitrate	5120 kbps
Maximum packet size	30 bytes (for $k = 9$)
Modulation	BPSK
Wind speed	15 m/s
Shipping level	1
Practical spreading	1.75
Interference model	DESERT "meanpower" model, considered at SINR
`TokenBus` Tk_{slot}	1.6 s (according to a 1200 m maximum network diameter)
`TDMA` t_g, T_f	0.15 s, 2.5 s

The acoustic physical layer computes the packet error probability starting from the attenuation and the channel noise models presented in [6] and implemented in DESERT in the `UwPhysical` module. The attenuation is used to compute the received power and, therefore, the SNR. Interference is also taken into account using the "meanpower" model present in DESERT to compute the Signal to Interference plus Noise Ratio (SINR). At the acoustic frequencies normally used for communication (in the range 1 kHz-100 kHz), the model in [6] considers wind speed and shipping activity as the main sources of noise: wind speed is set to 15 m/s, while the shipping activity (that simulates the presence of ships moving a few tens of kilometers from the network deployment) to 1. Practical spreading, that models the propagation geometry (2 for spherical spreading, 1 for cylindrical spreading, and values between 1 and 2 for the so called practical spreading, that is the most commonly found in practical scenarios), is set to 1.75, in fact the nodes move in a horizontal plane 200 m under the sea surface, hence we are neither in a very shallow water nor in a deep water scenario. The nodes transmit at a bitrate of 5120 bps with a power of 170 dB re 1 μPa on a band of 30 kHz around a carrier of 65 kHz, simulating the behavior of the modem Evologics 48-78 [24]. All simulation settings are summarized in Table 3. Finally, assuming a BPSK modulation scheme, the BER is computed with the standard formulas $BER = 0.5 \cdot \mathrm{erfc}(\sqrt{(SNR)})$, where erfc is the complementary error function. No coding is considered, hence the PER for a packet with size $S(k)$ can then be obtained with PER$= 1 - (1 - BER)^{8 \cdot S(k)}$. All the mentioned settings reflect realistic field conditions and device specifications, while the target positions to be reached by the nodes have been decided to have distances between the nodes such as the expected SNR would allow the activation of the algorithm for adaptive packet size: Figure 6 highlights how the PER changes with the transmission range and the ranging packet size $S(k)$, the results are plotted for each possible value of $k = 1 \ldots 9$ in a swarm of 10 nodes. The blue circles in the plot indicate the optimal value K as computed according to Eq. (7) for the adaptive procedure. We can observe how in phases 5 and 6 (where the maximum distance between two nodes ranges from 500 to 1000 m) K varies from 9 to 6.

5. Simulation Results

In this section we present and comment the results of the simulations performed with the DESERT framework. Numeric results summarizing the entire simulation cycle are presented in Table 4, showing the mean RMSE and the volume of ranging data transmitted by all the nodes; for each MAC, three policies have been tested: Full packets, B-SNR and AoI as presented in Section 3.4.

From the table we can see that adaptive packet policies were able to reduce transmitted data by 24% while obtaining, in the case of AoI policy, equal or better RMSE score than full packets. B-SNR instead provided

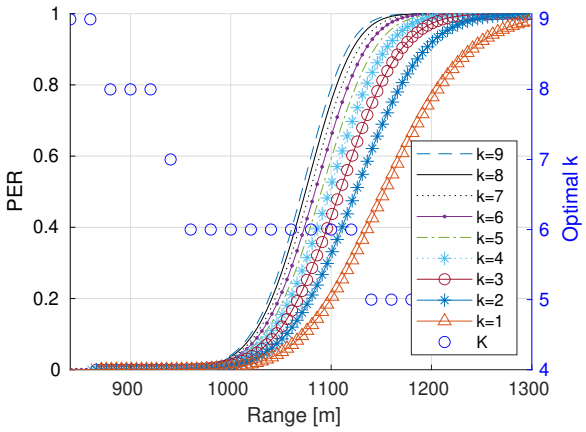

Figure 6: Packet error rate for $k = 1 \ldots 9$ and optimal K vs range.

Table 4: RMSE and bytes transmitted summary

	CSMA		Tokenbus		TDMA	
Policy	RMSE	TX	RMSE	TX	RMSE	TX
Full	11.94 m	352 KB	9.71 m	267 KB	11.88 m	131 KB
B-SNR	11.71 m	266 KB	10.82 m	248 KB	12.63 m	114 KB
AoI	10.66 m	266 KB	9.70 m	248 KB	11.83 m	114 KB

worse global results since when the nodes are in a fixed formation, it always privileges the same set of nodes which have the best SNR figures due to the proximity. Though B-SNR can prove useful in scenarios where the goal is to provide, during bad channel conditions, some minimum performance guarantees to a cluster of near nodes, in our scenarios it was outperformed by both AoI and Full policies, hence we exclude it from the analysis from here onward. Figures 7, 8 and 9, in fact, present more in detail the performance of Full and AoI policies for each of the MAC schemes. These plots represent the RMSE (defined in Eq. (8)) experienced by all the nodes during each movement phase: a logarithmic scale is used on the y-axis to better visualize the RMSE in the different phases. The mean value of each box is printed in the middle of the figure for easing the comparison.

In all the plots we can see that while the nodes are expanding radially the ranging error is greater then when the nodes are moving with a casual drift: this is expected since in the drift phase the distances between the nodes are bounded in a ±20 m range around a fixed point in the circumference. In both `CSMA-Aloha` (Figure 7) and `TDMA` (Figure 9), the RMSE is similar for all the three drift phases; for `TokenBus` (Figure 8) instead, since the update rate depends on the token rotation time, which itself depends on the distance between nodes, the RMSE starts with a very small value when the nodes are close, then increases with the mean distance. This characteristic makes TokenBus suitable as a MAC whenever it is desirable to have the error of the range measurements to scale proportionally with the distances and have the best accuracy when nodes operate close to each other. Comparing the plots of Full and AoI policies we can see that the adaptive mechanism kicks in during phases 5 and 6, where the higher distance between nodes causes lower SNR measures and thus high PER values, as already seen in the PER vs Range plot of Fig. 6. The adaptive policies prove to be more effective over `CSMA-Aloha` than `TDMA` and `Tokenbus` (which are non contention based) since smaller packets generate less packet loss due to collisions. In fact, while with `TDMA` and `Tokenbus` we did not observe collisions both with and without adaptation, with `CSMA-Aloha` we had 20990 collisions without adaptation and 17870 with adaptation, reducing the number of collisions by 15%. The result is that, for phase 6, i.e., the one mostly affected by channel adaptation, in `CSMA-Aloha` we also have an improvement of 15%. With `TDMA` and `Tokenbus` we have an improvement of 3% and 2%, respectively. Moreover, `TDMA` provides the worst performance for phases 0-4: this happens as the long timeframe (Tf = 2.5 s) increases the latency and, therefore, the AoI of the system even when the nodes are close. Nevertheless, although taking a shorter Tf would lead to better performance in the first phases of the mission, it would also cause an increasing number of collisions in phases 5 and 6, resulting in a worse RMSE. Indeed, Figure 10 depicts the effects of packet collisions with TDMA when Tf is 1.5 s: this exposes the rigidity of TDMA parameters in scenarios with moving nodes, while it could be an optimal choice whenever nodes have to keep a fixed formation. In such cases an optimized TDMA scheme such as the one proposed in [25] can maximize the throughput by using very low guard time values.

It worth mentioning that, even though this network architecture supports the transmission of other traffic types, the presence of a high traffic load would impact the ranging performance. From our simulations we assess that, for instance, with CSMA-Aloha the presence of an application layer that produces 64-byte packets according to a Poisson process with mean period T, would led to a deterioration of the RMSE, as compared to the one of Table 4, of respectively T=60 s: 8%, T=30 s: 20%, T=20 s: 39%, T=15 s: 67%, T=14 s: 93%.

6. Conclusion and Future Work

In this paper we described an implementation of a MAC-agnostic ranging protocol and reported exten-

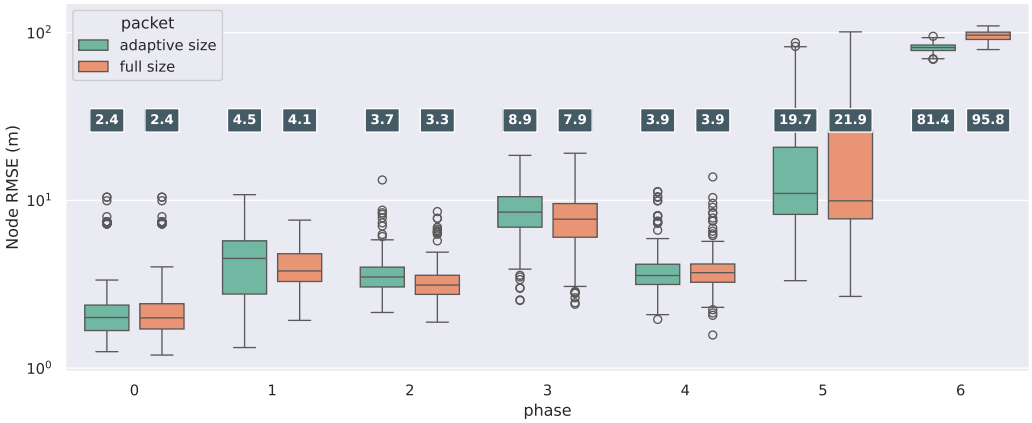

Figure 7: RMSE observed during the mission with `CSMA-Aloha` with full policy (orange) and adaptive AoI policy (green).

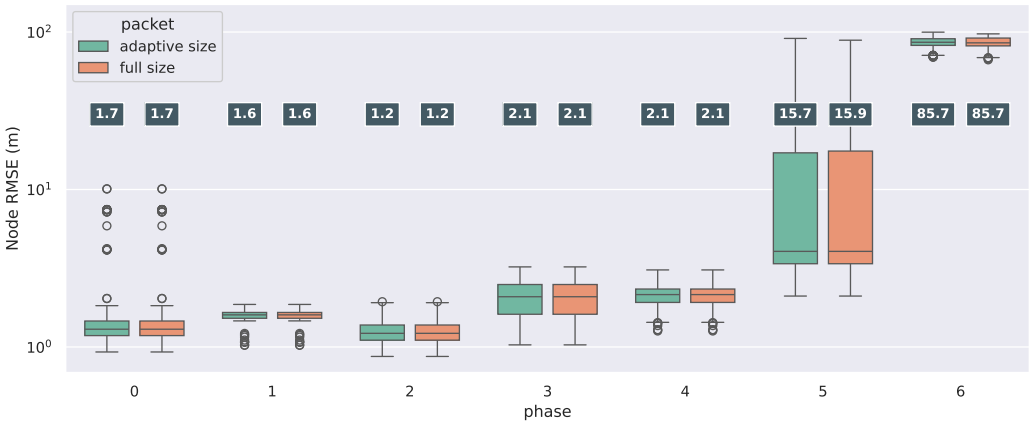

Figure 8: RMSE observed during the mission with `TokenBus` with full policy (orange) and adaptive AoI policy (green).

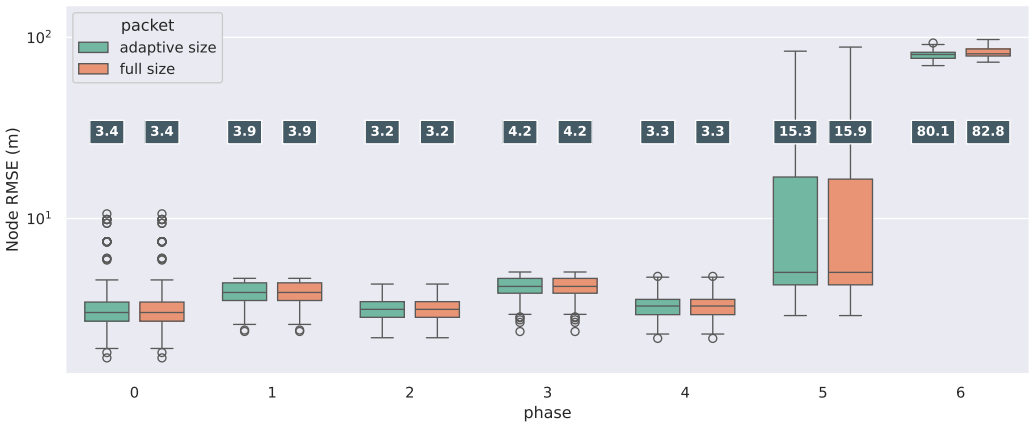

Figure 9: RMSE observed during the mission with `TDMA` with full policy (orange) and adaptive AoI policy (green).

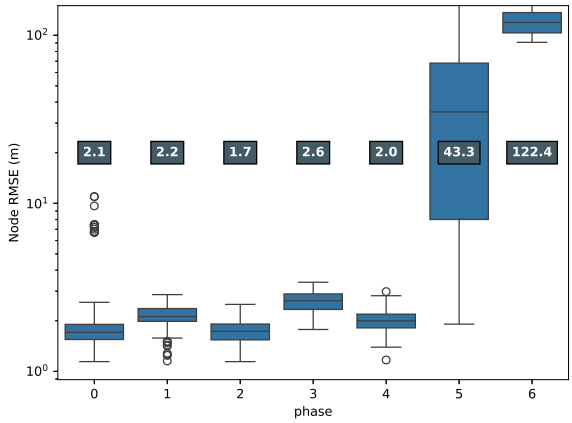

Figure 10: RMSE observed during the mission with a TDMA configuration with a low guard time and full policy: this speeds up the update cycle but causes a non negligible interference.

sive simulation results obtained over different MAC schemes, proving that it can be used with very different network deployments, including scenarios where contention-based MAC protocols are preferred, as well as scenarios where contention-free MAC protocols need to be used. The presented ranging protocol adapts its packet size according to the observed channel conditions, in order to maximize the goodput of the network and mitigate the interference. Moreover, the protocol selects the information entries to be inserted in each packet in such a way that the AoI is minimized: simulations of an AUV swarm scenario proved that this approach improves the system performance in terms of ranging precision and power consumption, allowing all AUVs in the swarm to know their distance from every other node in the network, thus allowing a better mission coordination. This implementation is publicly available in the `UwTDOARanging` module inside the DESERT Underwater framework, the tool than has been used in this paper to evaluate the protocol in simulations. `UwTDOARanging` will soon be tested in field experiments with EvoLogics and MODA [26, 27] acoustic modems, whose drivers are already integrated in DESERT Underwater.

Acknowledgement

This work has been partially supported by the Italian General Directorate of Naval Armaments (NAVARM) and the Italian National Plan for Military Research (PNRM) (contract 20593), by the European Union - FSE REACT EU, PON Research and Innovation 2014-2020 (DM 1062/2021), and by the Italian National Recovery and Resilience Plan (NRRP) of NextGenerationEU, as part of the partnership on "Telecommunications of the Future" (PE0000001 - program "RESTART").

References

[1] BlueROV2, Last time accessed: Oct. 2023.
URL `https://bluerobotics.com/store/rov/bluerov2/`

[2] Loco-auv, Last time accessed: Oct. 2023.
URL `https://loco-auv.github.io/`

[3] H. Dol, EDA-SALSA: Towards smart adaptive underwater acoustic networking, in: IEEE/MTS OCEANS, Marseille, France, 2019. doi:10.1109/OCEANSE.2019.8867361.

[4] K.G. Kebkal, O.G. Kebkal, E. Glushko, V.K. Kebkal, L. Sebastião, A. Pascoal, J. Gomes, J. Ribeiro, H. Silva, M. Ribeiro, and G. Indivery, Underwater acoustic modems with integrated atomic clocks for one-way travel-time underwater vehicle positioning, in: Proc. UACE, Skiathos, Greece, 2017.

[5] G. Ferri, R. Petroccia, T. Fabbri, A. Faggiani, A. Tesei, A Network Navigation System With Opportunistic Use of One-Way and Two-Way Acoustic Ranging: the DANS20 Experience, in: IEEE/MTS OCEANS, San Diego – Porto Vitual Oceans, 2021. doi:10.23919/OCEANS44145.2021.9706011.

[6] M. Stojanovic, On the relationship between capacity and distance in an underwater acoustic communication channel, ACM SIGMOBILE Mobile Computing and Communications Review 11 (4) (2007) 34–43. doi:10.1145/1347364.1347373.

[7] I. F. Akyildiz, D. Pompili, T. Melodia, Underwater acoustic sensor networks: Research challenges, Ad Hoc Networks 3 (2005) 257–279.

[8] J. Heidemann, M. Stojanovic, M. Zorzi, Underwater sensor networks: applications, advances and challenges, Philosophical Transactions of the Royal Society A: Mathematical, Physical and Engineering Sciences 370 (1958) (2012) 158–175.

[9] A. Pal, F. Campagnaro, K. Ashraf, M. R. Rahman, A. Ashok, H. Guo, Communication for underwater sensor networks: A comprehensive summary, ACM Transactions on Sensor Networks 19 (22) (2022) 1–44. doi:https://doi.org/10.1145/3546827.

[10] A. Montanari, F. Campagnaro, M. Zorzi, One-and Two-Way Travel Time Ranging in Underwater Acoustic Mobile Networks., in: The 16th International Conference on Underwater Networks & Systems (WUWNet'22), November 14–16, 2022, Boston, 2022. doi:10.1145/3567600.3568156.

[11] K. Kredo II, P. Djukic, P. Mohapatra, STUMP: Exploiting Position Diversity in the Staggered TDMA Underwater MAC Protocol, in: IEEE INFOCOM 2009, pp. 2961–2965. doi:10.1109/INFCOM.2009.5062267.

[12] T. C. Furfaro, J. Alves, An application of distributed long baseline — node ranging in an underwater network, in: IEEE Underwater Communications and Networking (UComms), 2014, pp. 1–5. doi:10.1109/UComms.2014.7017126.

[13] T. Stojimirovic, B.-C. Renner, Accuracy of TWR-Based Ranging and Localization in Mobile Acoustic Underwater Networks, in: IEEE Underwater Communications and Networking Conference (UComms), 2021, pp. 1–5. doi:10.1109/UComms50339.2021.9598074.

[14] S. A. H. Mohsan, Y. Li, M. Sadiq, J. Liang, M. A. Khan, Recent Advances, Future Trends, Applications and Challenges of Internet of Underwater Things (IoUT): A Comprehensive Review, Journal of Marine Science and Engineering 11 (1) (2023). doi:10.3390/jmse11010124.
URL `https://www.mdpi.com/2077-1312/11/1/124`

[15] F. Campagnaro, F. Steinmetz, B.-C. Renner, Survey on low-cost underwater sensor networks: From niche applications to everyday use, Journal of Marine Science and Engineering 11 (1) (2023). doi:10.3390/jmse11010125.
URL https://www.mdpi.com/2077-1312/11/1/125

[16] O. Kebkal, K. Kebkal, R. Bannasch, Long-baseline Hydroacoustic positioning using D-MAC communication protocol, in: 2012 Oceans - Yeosu, 2012, pp. 1–7. doi:10.1109/OCEANS-Yeosu.2012.6263529.

[17] V. Ludovico, J. Gomes, J. Alves, T. C. Furfaro, Joint localization of underwater vehicle formations based on range difference measurements, in: IEEE Underwater Communications and Networking (UComms), 2014, pp. 1–5. doi:10.1109/UComms.2014.7017127.

[18] O. Vikhrova, F. Chiariotti, B. Soret, G. Araniti, A. Molinaro, P. Popovski, Age of information in multi-hop networks with priorities, in: GLOBECOM 2020 - 2020 IEEE Global Communications Conference, 2020, pp. 1–6. doi:10.1109/GLOBECOM42002.2020.9348175.

[19] DESERT: Design, simulate, emulate and realize test-beds for underwater network protocols, Last time accessed: Oct. 2023.
URL https://desert-underwater.dei.unipd.it/

[20] F. Campagnaro, R. Francescon, F. Guerra, F. Favaro, P. Casari, R. Diamant, M. Zorzi, The DESERT Underwater framework v2: Improved capabilities and extension tools, in: IEEE Underwater Communications and Networking (UComms), Lerici, Italy, 2016.

[21] J. Śliwka, R. Petroccia, A. Munafò, V. Djapic, Experimental evaluation of net-lbl: An acoustic network-based navigation system, in: IEEE/MTS OCEANS 2017 - Aberdeen, 2017, pp. 1–9. doi:10.1109/OCEANSE.2017.8084794.

[22] A. Munafò, G. Ferri, An acoustic network navigation system, Journal of Field Robotics 34 (7) (2017) 1332–1351. doi:https://doi.org/10.1002/rob.21714.

[23] IEEE standard for information processing systems – local area networks –part 4: Standard for token-passing bus access method and physical layer specifications, ANSI/IEEE Std 802.4-1990 (Revision of ANSI/IEEE 802.4-1985) (Adopted by ISO/IEC and redesignated as ISO/IEC 8802-4: 1990) (1990) 1–278doi:10.1109/IEEESTD.1990.7229456.

[24] EvoLogics Underwater Acoustic Modems, https://evologics.de/acoustic-modems, Last time accessed: Sep. 2023.

[25] Jianyu Zhang, Filippo Campagnaro, Michele Zorzi, "Spatial-reuse TDMA for Large Scale Underwater Acoustic Multi-hop Grid Networks", in: OCEANS 2023 - Limerick, Limerick, Ireland, 2023.

[26] F. Campagnaro, R. Francescon, E. Coccolo, A. Montanari, M. Zorzi, A software-defined underwater acoustic modem for everyone: Design and evaluation, IEEE Internet of Things Magazine 6 (1) (2023) 102–107. doi:10.1109/IOTM.001.2200221.

[27] E. Coccolo, F. Campagnaro, D. Tronchin, A. Montanari, R. Francescon, L. Vangelista, M. Zorzi, Underwater acoustic modem for a morphing distributed autonomous underwater vehicle (MODA), in: IEEE/MTS OCEANS - Chennai, 2022, pp. 1–8. doi:10.1109/OCEANSChennai45887.2022.9775308.